A Slow Crack Growth Model for High-Density Polyethylene under Thermal and Chemical Environment

By

Hyun Young Nam

B.S., Kyungpook National University, 2021

Thesis

Submitted in partial fulfillment of the requirements for the Degree of Master of Science in the School of Engineering at Brown University

PROVIDENCE, RHODE ISLAND

MAY 2023

AUTHORIZATION TO LEND AND REPRODUCE THE THESIS

As the sole author of this thesis, I authorize Brown University to lend it to other institutions for the purpose of scholarly research.

Date 04/30/2023 Hyun-Young Nam

Hyun Young Nam, Author

I further authorize Brown University to reproduce this thesis by photocopying or other means, in total or in part, at the request of other institutions or individuals for the purpose of scholarly research.

Date 04/30/2023 Hyun-Young Nam

Hyun Young Nam, Author

This thesis by Hyun Young Nam is accepted in its present form by the Department of Engineering as satisfying the thesis requirement for the degree of Master of Science

Date 04/29/2023

Prof. Vikas Srivastava, Advisor

Approved by the Graduate Council

Date __________

Thomas A. Lewis, Dean of the Graduate School

Acknowledgments

I would like to start by acknowledging my advisor, Prof. Vikas Srivastava. It was not easy for me to adjust myself to the United States at first, and his effort to help me was crucial to complete two years of graduate studies at Brown. Not only did his kind personality, but also his guidance motivated me to shape my attitude as an independent researcher and go further to successfully complete my graduate study.

I would also like to thank my undergraduate advisor Prof. Gunwoo Noh in South Korea, who lead me to the researcher's life. I will never forget that he got me out of the very bottom of my life and will respond to his favor by gratefully and humbly taking this journey.

During my time at Brown, I have met great friends and I am very thankful for their support and friendship. I am particularly grateful to Michael Daniti for being my first and best friend at Brown and helping me whenever I got in trouble; to Tom Pilvelait, Srijan Neogi, and Zahra Ahmed for joyful chat and hanging out; to Kevin LoGiudice for hilarious and interesting jokes; to Sijun Niu for being a whiskey tasting friend; to Francesca Abulancia for making me talk more in the office; and to Aditya Konale for the research conversation. I will remember the fun days in Barus and Holley 750 until the end of my life.

Finally, I would like to thank my friends and family in South Korea. Without their warm support, I would never get this tough journey done.

Contents

List of Figures

List of Tables

ABSTRACT

High-density polyethylene (HDPE) is a widely used thermoplastic polymer with application as the material for pipeline transport systems. Due to the long-term, low-stress conditions of pipelines and the viscoelastic properties of HDPE, it is inevitable for the material to undergo a slow crack growth (SCG) failure mechanism. In addition to the applied loads, SCG is also affected by the chemical and thermal environments of the transport system. It is therefore crucial to develop a SCG model to more accurately predict the long-term failure of HDPE by taking into account the chemical and thermal effects. Experimental data was retrieved from literature of full notch creep tests (FNCT) performed at various temperatures and under chemical exposure to an environmental stress cracking (ESC) agent to develop this SCG model. The HDPE specimen time to failure (t_f) data was extracted in addition to the test specimen elongation (l), which was then converted to crack-tip opening distance (COD, δ). The viscoelastic behavior of HDPE was captured through a Maxwell model consisting of four branches and a Prony series type model with parameters calibrated using the experimental data. Computational simulations were performed by implementing the model in a commercial finite element analysis software ABAQUS to obtain the mathematical relationship between elongation and COD. The COD data from different thermal and chemical exposure conditions to develop the SCG model. The model accurately predicted the long-term structural failure of HDPE observed in another data set used as validation obtained from literature. This model has application in the design and maintenance of HDPE pipelines for the transport system.

1 Introduction

1.1 High-Density Polyethylene

High-density polyethylene (HDPE) is a semi-crystalline thermoplastic polymer composed of crystalline lamella regions and amorphous regions with inter-lamellar tie-molecule links dispersed throughout (1). HDPE is widely used in the transport industry as the material for pipelines due to being inexpensive, reliable in the long-term, versatility, and high integrity (2). Polymers are beginning to replace heavier materials like glass and metal in many industrial applications. A primary material advantage to HDPE is its long service life. This can be negatively impacted by not only the stress applied on the pipe but also by environmental factors. Pipelines may operate under high temperatures in the transport of natural gas. The pipes can also be responsible for the transportation of aggressive chemicals. Therefore, it is critical to investigate the failure mechanism of HDPE under thermal and chemical exposure to accurately predict its longevity in practical applications.

1.2 Slow Crack Growth

The long-term failure of polyethylene is governed by a slow crack growth (SCG) mechanism. SCG describes a brittle mode of polymer failure that is responsible for the reduced service time in industrial applications. Failure of HDPE due to SCG will occur over long time periods and low stresses (3; 4). In SCG, low stress can be defined as stress well below the yield stress of the material. Figure 1 shows the hoop stress versus time to failure plot in which different modes of failure are observed in polyethylene at decreasing levels of hoop stress (6). Region A represents the ductile failure range at high hoop stress, region B represents a quasi-brittle failure at decreasing hoop stress, and region C represents brittle failure at low hoop stress. Because plastic deformation will only localize near the crack tip, linear elastic fracture mechanics (LEFM) can be used for SCG modeling (5; 6; 7). Referring to the depiction of SCG failure mechanism in Figure 2, the zone of plastic deformation lies between the craze region and the bulk material. LEFM can describe the behavior at the crack tip due to its linear elastic material behavior and small-scale plasticity, allowing for the entire specimen to be considered as linearly elastic because the small-scale inelasticity can be neglected (8).

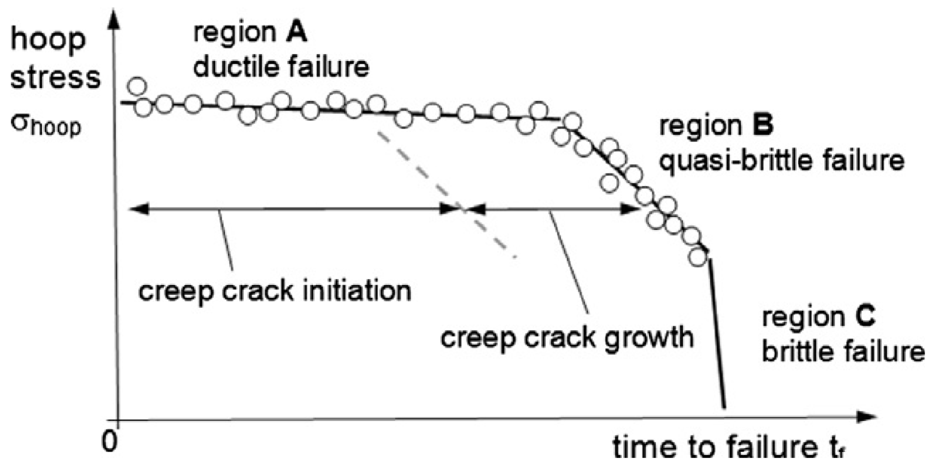

Figure 1: Hoop stress versus time to failure (6).

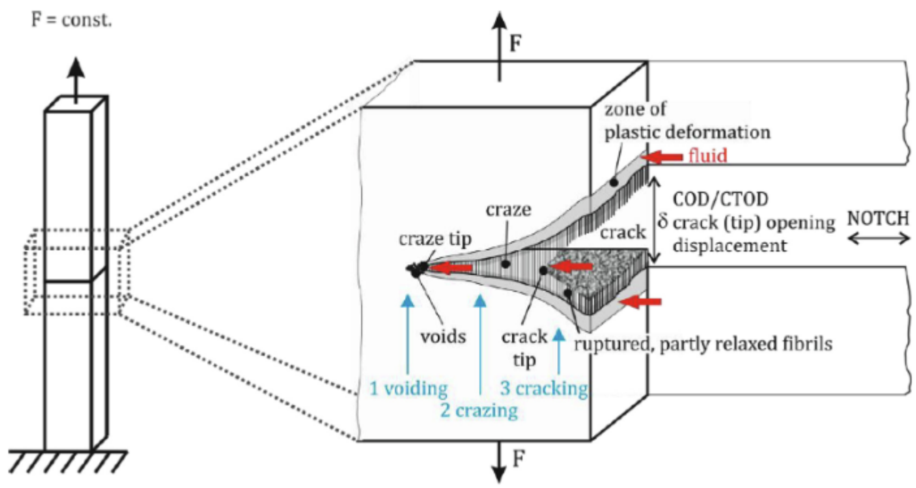

Figure 2: A schematic representation of the craze and crack growth (7).

1.3 Experiments for Environmental Stress Cracking in HDPE

Two types of HDPE were investigated by Schilling, et al. under various thermal and chemical conditions: AGUV and 5021DX (9). AGUV HDPE is used for high-performance applications and is produced using a gas phase polymerization method (7). 5021DX is the commercially available type of HDPE produced through loop polymerization (7). Only AGUV HDPE experimental data was considered for the current work. Full-notch creep tests (FNCT) were performed by Schilling in low-stress regimes, less than half of material yield stress of 24 MPa. FNCT utilize a symmetric notch around all four edges of the test specimen about the thickness. Single-edge notch test (SENT) only has a notch initiated along one edge of the thickness and the Pennsylvania notch test (PENT) has a notch about 3 edges of the test specimen thickness (10). FNCT sample geometry has accelerated experiment time in comparison to other test methods because the notch is present along all edges of the sample thickness. The experimental measure in this work was the elongation of the specimen (l) over time until failure and it was extracted by using the data analysis software OriginPro. Experimental temperatures were 30°C to 70°C in 10°C increments for extracted data of time to failure and 30°C to 50°C in 10°C increments for extracted data of elongation. Experimental chemical exposures were water and Arkopol, an environmental stress cracking (ESC) agent known to accelerate SCG in polyethylenes according to the ASTM D1693 specification (11). Arkopol is shown to produce the same type of brittle failure observed in gas pipelines after long service times (12) (13). The considered stress regimes were varied from 8 MPa to 12 MPa in increments of 1 MPa, which is much less than the material yield stress of 24 MPa. In order to model the SCG failure mechanism, the two important criteria are crack-tip opening distance (COD, δ) and time to failure (t_f). The elongation data from Schilling's experiments must therefore be converted to COD data for modeling of the SCG failure mechanism. Visualization of the COD term is shown in Figure 2 as the displacement of the crack-tip opening in the same direction as the applied low stress (7). Also of interest in this diagram is the depiction of the craze-crack phenomenon, in which crazing (a collection of very fine cracks) occurs due to the localized stress at the crack tip (14).

1.4 Problem Description and Solution Strategy

The objective of the current study is to devise an accurate SCG model that can explain the thermal and chemical effects. In this study, a new SCG model was developed by modifying one developed by Brown and Lu to incorporate thermal and chemical exposure terms (14). Model calibration was conducted using the experimental data of Schilling, in which chemical exposure, applied low stress, and thermal conditions were varied (7). SENT experimental data from Brown and Lu were used to validate the developed model (15).

2 Computational Simulations

2.1 Prony Series Parameters

HDPE is a viscoelastic material, so we used a Maxwell model with 4 branches to capture its constitutive behavior. For that purpose, the strain data was extracted from the experiment of Amjadi and coworkers (16). The extracted strain data can be converted to the Young's modulus by using equation 1.

$$E(t) = \frac{\sigma}{\epsilon(t)} \tag{1}$$

where $E(t)$ is Young's modulus, σ is a fixed applied load of 13MPa and $\epsilon(t)$ is extracted strain. The strain data from (16) is shown in Figure 3(a) and the converted Young's modulus data is shown in Figure 3(b).
We then used a Prony series to fit the modulus data shown in Figure 3(b) and calibrated the time dependent parameters of the Maxwell model (E_i and τ_i). For that purpose, we used the following creep expression to fit the modulus data:

$$E(t) = E_\infty + \sum_{i=1}^{n} E_i \cdot exp(-\frac{t}{\tau_i}) \tag{2}$$

where $E_\infty = 1100\text{MPa}$ is a long-term Young's modulus once the material is totally relaxed (16), n is the number of branches in Prony series, τ_i and E_i are the relaxation time and Young's modulus of ith branch of Prony series, respectively.
The fraction of Young's modulus in equation 3 was used when applying the Prony series in the Abaqus.

$$g_i = \frac{E_i}{E(t)} \tag{3}$$

The parameters used in Abaqus are summarized in Table 1.

The experimental data used for getting Prony series constants was done with a dog bone-shaped sample without an initial crack so that we can minimize the

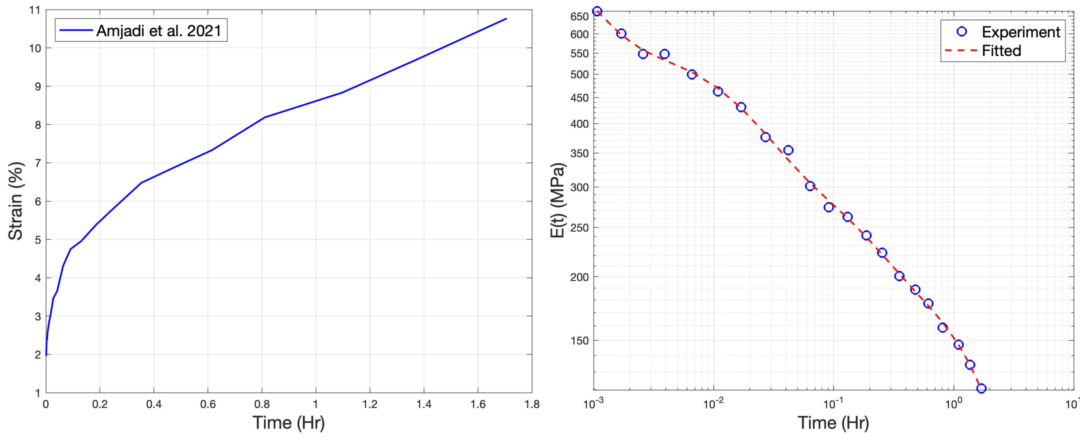

(a) extracted strain data (b) calculated Young's modulus

Figure 3: MATLAB fitting to get Prony series parameters

i	g_i	τ_i
1	0.2296	2.54
2	0.1132	72.6
3	0.0642	566.3
4	0.1038	10752

Table 1: Prony series parameters for finite element simulation.

effects of geometry condition and focus on its viscoelastic behavior.

2.2 Simulations

The geometry used for simulation is described in Figure 4 with the dimension of 6mm × 6mm × 30mm (Length × Width × Height). The same type of specimen in Schilling's experiments, the FNCT specimen, is used, however, we considered a gauge length of 30mm.

Figure 5 demonstrates the boundary condition of the FNCT sample, while Figure 6 shows the displacement contour of the sample after simulation. The bottom of the specimen is fixed and three data sets were extracted after simulation: COD bottom, COD top, and total elongation of the specimen.

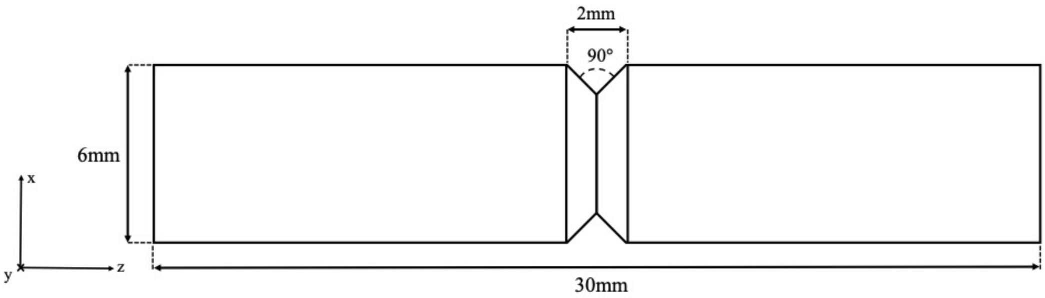

Figure 4: Geometry of FNCT sample

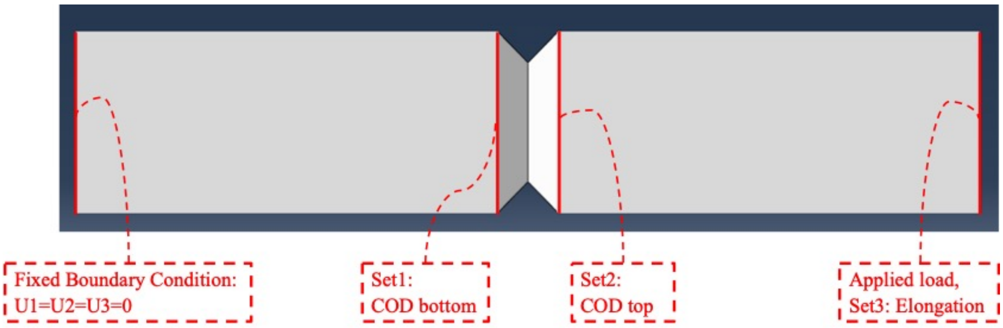

Figure 5: Boundary condition of FNCT sample

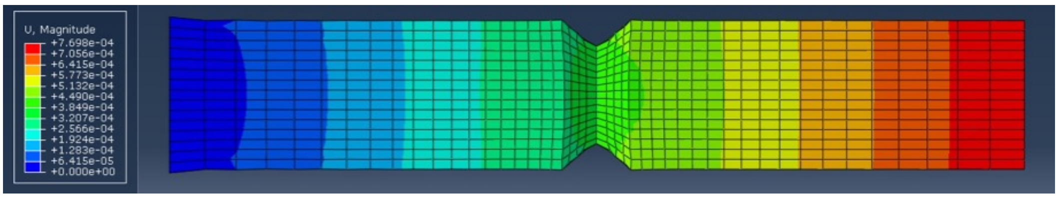

Figure 6: Displacement, U(m) in ABAQUS simulation

The COD is calculated by using equation 4.

$$COD = COD_{top} - COD_{bottom} \tag{4}$$

The damage was not considered in the simulations since we assumed that the absence of damage doesn't affect the relationship between elongation and COD. We conducted separate simulations with various initial crack depths (0.5mm, 0.75mm, 1mm, 1.25mm, and 1.5 mm) to investigate the influence of the initial crack depth on the relationship between elongation and COD. Figure 7 represents the assumption in the simulation. The red line is the simulation results without considering the damage, while the blue line is the estimated results when considering the damage.

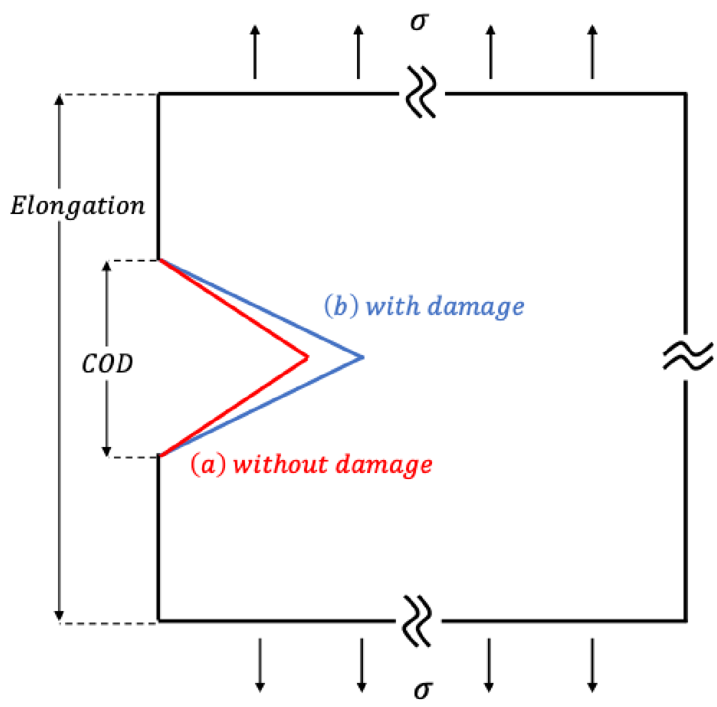

Figure 7: Assumption in simulation

The simulations were conducted with various stress (8, 9, 10, 11, 12MPa) and initial crack depth (0.5, 0.75, 1, 1.25, 1.5 mm).

2.3 Converted Data

The results in simulations show that the elongation is a linear function of the COD as expressed in equation 5.

$$l = (slope) \cdot \delta \tag{5}$$

The slope in equation 5 depends on the initial crack depth, and its dependence was fitted in MATLAB as shown in Figure 8. After normalizing the elongation and COD, the final relationship between elongation and COD can be written in dimensionless equation 6.

$$(\frac{\delta}{w}) = 1.55(\frac{a}{w})^{1.174}(\frac{l}{w}) \tag{6}$$

where w is the width and a is the initial crack depth.

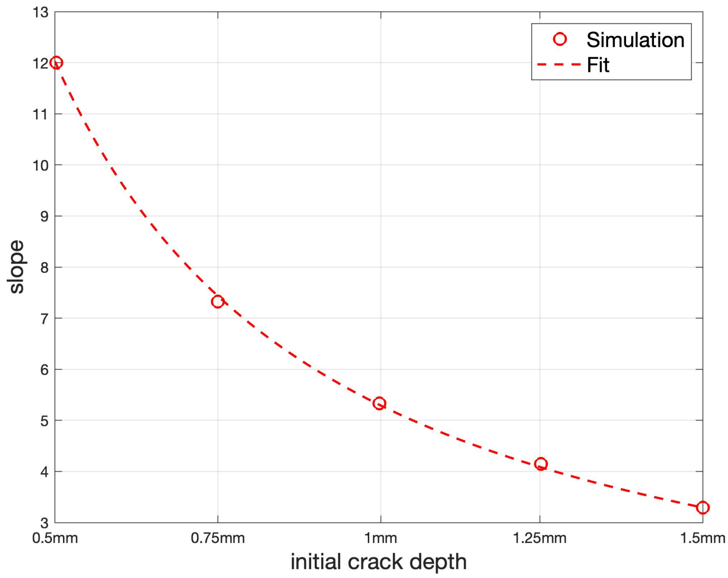

Figure 8: Relationship between elongation and COD: slope versus initial crack depth

When the initial crack depth is fixed, the elongation shows a linear relation with COD. In this study, only one case of initial crack depth is considered which is $a =$ *1mm*. Thus, equation 7 can be expressed as below.

$$(\frac{\delta}{w}) = 0.1876(\frac{l}{w}) \tag{7}$$

Figure 9 shows the general COD versus time curve. The region of interest is the slope of the curve in the highlighted area.

The equation for calculating the COD rate is given as

$$\dot{\delta} = \frac{\delta_b - \delta_0}{t_b} \tag{8}$$

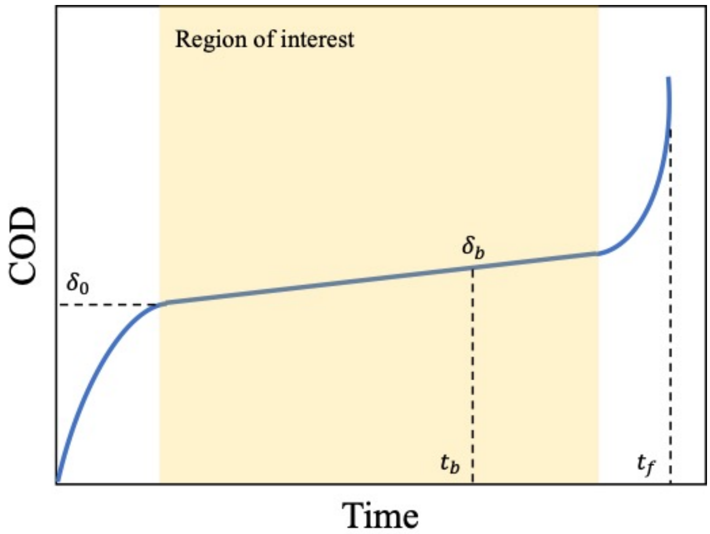

Figure 9: COD rate

where $\dot{\delta}$ is COD rate, δ_0 is initial COD, δ_b is COD for crack initiation, and t_b is the corresponding time which must be in from 0.2 to 0.8 of time to failure t_f.

3 Slow Crack Growth Model

3.1 Previous SCG Model

The previous slow crack growth model developed by Brown and his coworker (14) starts with the equation for force balance as shown in Figure 10.

$$\sigma_B A_0 = \sigma_F A \tag{9}$$

where σ_F is the average stress on fibril and σ_B is the stress at boundary of craze. Also, A_0 and A represent the area where boundary and fibril stress is applied, respectively. As shown in Figure 10, the relationship between initial stress and primordial thickness can be written as the equation below, which is derived from the assumption that the craze originates from the primordial volume.

$$A\delta_0 = A_0 d_0 \tag{10}$$

By combining equations 9 and 10, the stress at fibril can be defined as

$$\sigma_F = \frac{\sigma_Y \delta_0}{d_0} \tag{11}$$

The assumption of the previous study is that $\dot{\delta}$ is a linear function of σ_F as below since it is very slow enough to mimic Newtonian fluid as expressed in equation 12

$$\frac{\dot{\delta}}{\delta_0} = \frac{\sigma_F}{\eta} \tag{12}$$

where η is viscosity and $\boldsymbol{\delta_0}$ is the initial COD.

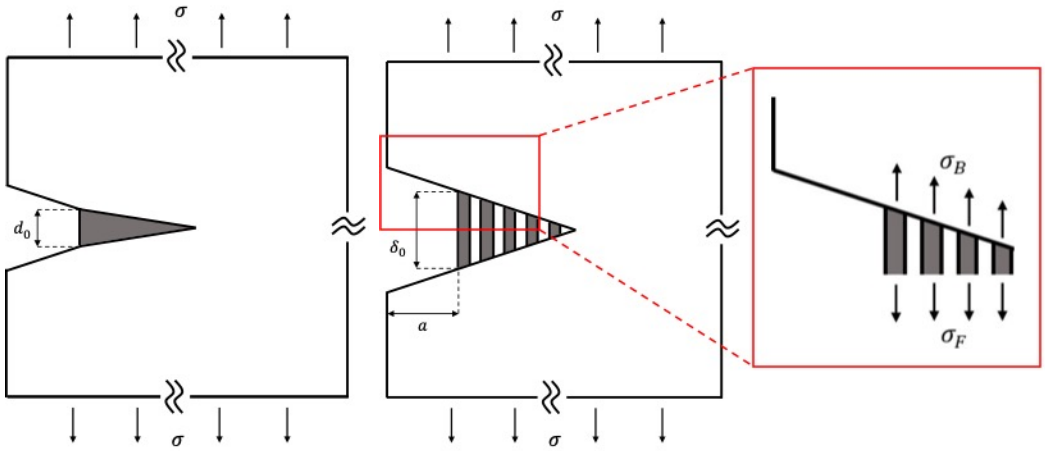

(a) Primordial (b) After crazing

Figure 10: Craze in HDPE

From the Dugdale theory for plane strain condition as derived in the reference paper (17), the initial COD can be represented as

$$\delta_0 = \frac{K^2}{E\sigma_c}(1-\nu^2) \tag{13}$$

where $\boldsymbol{\delta_0}$ is the initial COD, E is Young's modulus, ν is Poisson's ratio, σ_c is crazing stress that is typically same with yield stress (15), and K is stress intensity factor in tensile mode as shown in equation 14

$$K = Y\sigma\sqrt{\pi a} \tag{14}$$

where Y is geometry factor, σ is applied stress, and a is the initial crack depth. Combining equations 11-14, Brown's SCG model can be represented as equation 15.

$$\dot{\delta} = \frac{\sigma_Y Y^4(1-\nu^2)^2\sigma^4 a^2}{\eta d_0 E^2 {\sigma_c}^2} \tag{15}$$

While this SCG model shows well-matched results with their experiments, it doesn't explain the chemical and thermal effect. Another limitation in Brown's SCG model is flexibility in stress term; although the stress term, σ^{m}, has a fixed exponent of 4,

m depends on the type of polyethylene resins and has a various range of value (14).

3.2 Proposed SCG model

The proposed SCG model starts with modifying equation 12. The chemical degradation can accelerate the growth of crack, which means COD rate in equation 12 may not be a linear function of fibril stress. With Brown's SCG model (14), the phenomenon that chemical degradation accelerates SCG cannot be captured, and a new assumption should be required to explain chemical effects in SCG; the assumption in this study is that the COD rate is a non-linear function of fibril stress so that the proposed model can have more flexibility in stress term to accurately fit the experimental data with chemical effects. To be more specific, we used the following form of COD rate in this study:

$$\frac{\dot{\delta}}{\delta_0} = \frac{\sigma_2}{\eta}(\frac{\sigma_F}{\sigma_1})^{m/2-1} \tag{16}$$

where m is a exponential constant, σ_1 and σ_2 are stress-like fitting parameters having unit of Pa.

After combining equations 11, 13, 14, and 16, the exponential term in the Arrhenius equation was multiplied for describing the effect of the thermal environment (14). Additionally, chemical exposure constant κ is added in the proposed SCG model for explaining chemical effects as well. The final form of the slow crack growth model including chemical and thermal effects:

$$\dot{\delta} = \frac{\sigma_1\sigma_2 d_0}{\sigma_Y \eta} \cdot \kappa \cdot (\frac{\sqrt{(1-\nu^2)\pi a}Y\sigma}{\sqrt{E\sigma_1 d_0}})^m \cdot \exp(-\frac{Q}{RT}) \tag{17}$$

$$t_f = \frac{\sigma_Y \eta x}{\sigma_1\sigma_2 d_0} \cdot \frac{1}{\kappa} \cdot (\frac{\sqrt{(1-\nu^2)\pi a}Y\sigma}{\sqrt{E\sigma_1 d_0}})^{-n} \cdot \exp(\frac{Q}{RT}) \tag{18}$$

The description of parameters in the proposed SCG model is shown in Table 2.

Parameter	Description	Parameter	Description
$\boldsymbol{\sigma_1}$, $\boldsymbol{\sigma_2}$	fitting parameters (Pa)	σ	applied stress (Pa)
E	Young's modulus (Pa)	ν	Poisson's ratio
Y	geometry factor	a	initial crack depth (m)
η	viscosity (Pa·s)	d_0	primordial thickness (m)
Q	activation energy (J/mol)	R	universal gas constant (J/mol·K)
T	temperature (Kelvin)	κ	chemical exposure constant
x	unit correction factor (m)	m, n	exponent

Table 2: Parameters in the proposed SCG model

The chemical exposure constant and unit correction factor varies with the type of chemical as summarized in Table 3.

Parameter	Water	Parameter	Arkopal
κ_{water}	9	κ_{Arkopal}	1
x_{water}	3.26e-14 (m)	$\text{x}_{\text{Arkopal}}$	1.63e-14 (m)

Table 3: Chemical exposure constant and unit correction factor

Young's modulus is 850MPa, Poisson's ratio is 0.45, initial crack depth is 1mm, fitting parameters σ_1 is 152kPa and σ_2 is 9MPa. For the geometry factor for FNCT, Y=3 is used so that the stress intensity factor must be higher than the threshold stress intensity of 0.08 MPa $\cdot$ m$^{1/2}$ (15). The activation energy is 100kJ/mol for Arkopal as specified in (14), and a slightly higher value, 110kJ/mol, was used for Water, the universal gas constant is 8.3145kJ/mol·K, and exponents m is 10 and n is 5. The viscosity can be calculated from the following equation

$$\eta = \frac{\sigma_Y \delta_0^2}{d_0 \dot{\delta}} \tag{19}$$

where δ_0 is gotten from equation 13 once the stress intensity factor is fixed, and d_0 can be calculated from equation 20 which represents the porosity of the craze (14).

$$1 - \frac{d_0}{\delta_0} = 0.5 \tag{20}$$

The calculated initial COD is $\delta_0 = 70\mu$m, primordial thickness is $d_0 = 35\mu$m, and the viscosity is $1.13 \times 10^{10}\text{Pa} \cdot \text{s}$.

Additionally, COD at failure can be defined as the crack-tip opening distance just before the specimen is separated into two parts, and it can be represented by combining equations 17 and 18,

$$\delta_f = \dot{\delta} \cdot t_f = x\left(\frac{\sqrt{(1-\nu^2)\pi a} Y \sigma}{\sqrt{E \sigma_1 d_0}}\right)^{m-n} \tag{21}$$

Even though the chemical and temperature terms vanished in equation 21, it is hard to say there is no influence from chemical exposure and temperature since primordial thickness can be different with various thermal conditions. Rather, it could be said that the influence of chemical exposure and temperature is minimized. The proposed model and experimental data for $\dot{\delta}$ with various stress and temperature were demonstrated in Figures 11 and 12.

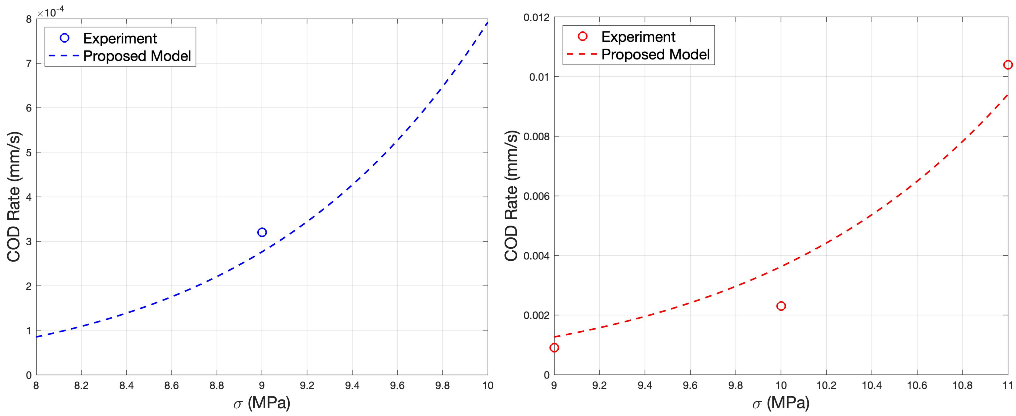

(a) Water (b) Arkopal

Figure 11: COD rate at 50°C: Proposed model and Experimental data (9)

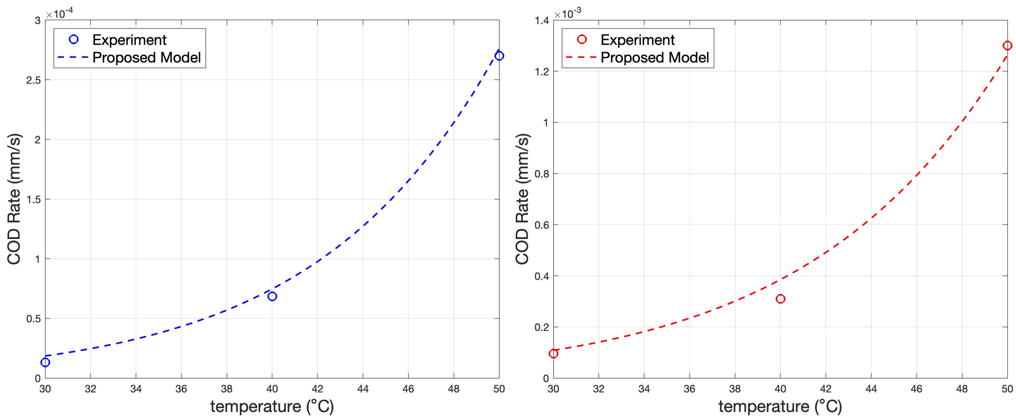

(a) Water (b) Arkopal

Figure 12: COD rate at 9MPa: Proposed model and Experimental data (9)

In the experiment of (9), they found a ductile to brittle transition at around 11 MPa for water and approximately 9.5 MPa for Arkopal (Figure 13), below which brittle fracture occurs. So we considered stress below these values for our SCG model.

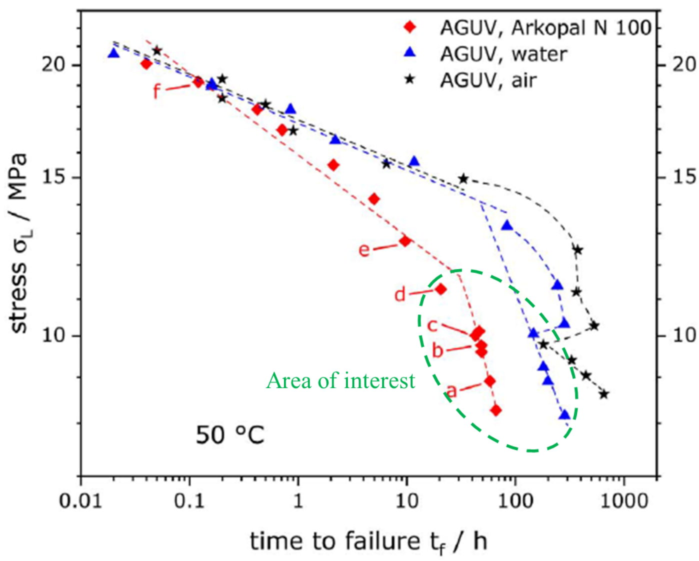

Figure 13: Area of interest that SCG occurs in the experiment of Schilling (9)

Figures 14 and 15 show the proposed model and experimental data for the time to failure.

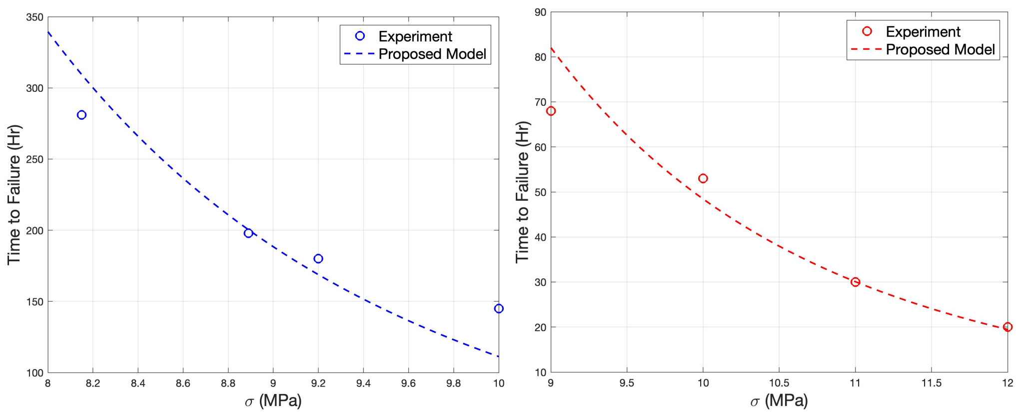

(a) Water (b) Arkopal

Figure 14: Time to failure at 50°C: Proposed model and Experimental data (9)

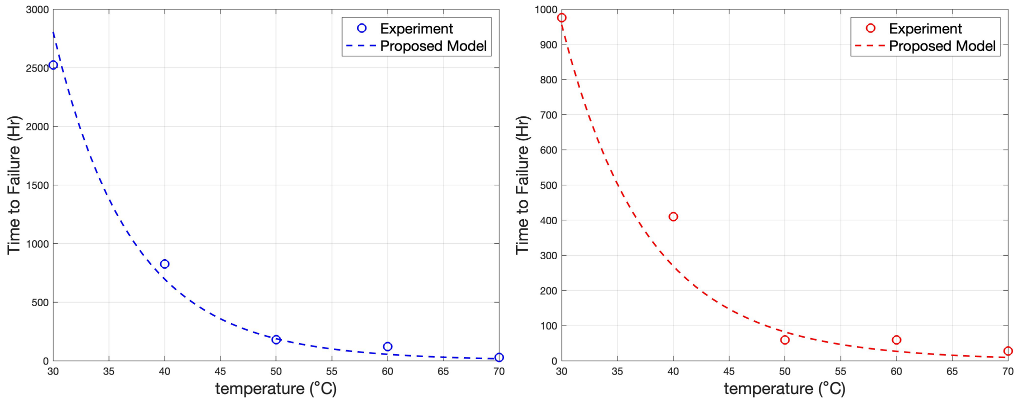

(a) Water (b) Arkopal

Figure 15: Time to failure at 9MPa: Proposed model and Experimental data (9)

Figures 16 and 17 show the COD rate and time to failure in a three-dimensional contour, where the black dot represents experimental data (9) and the contour plot represents the proposed model. Both results of COD rate and time to failure show a good agreement with experimental data.

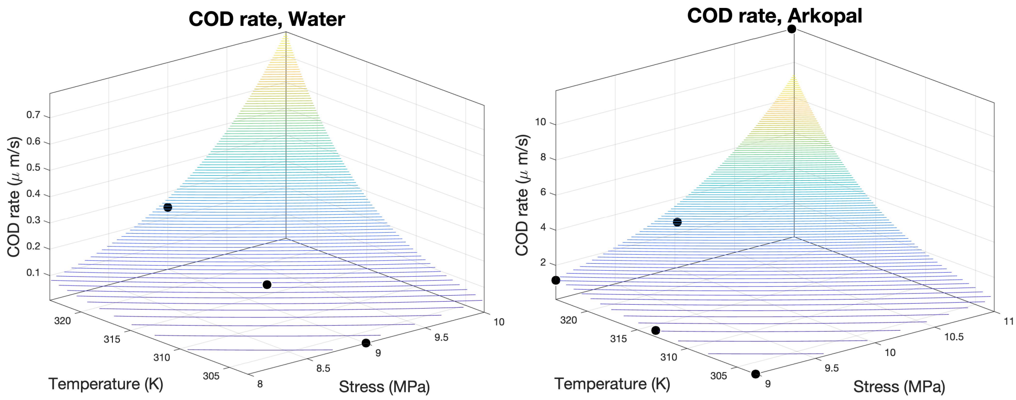

(a) Water (b) Arkopal

Figure 16: 3D contour of COD rate

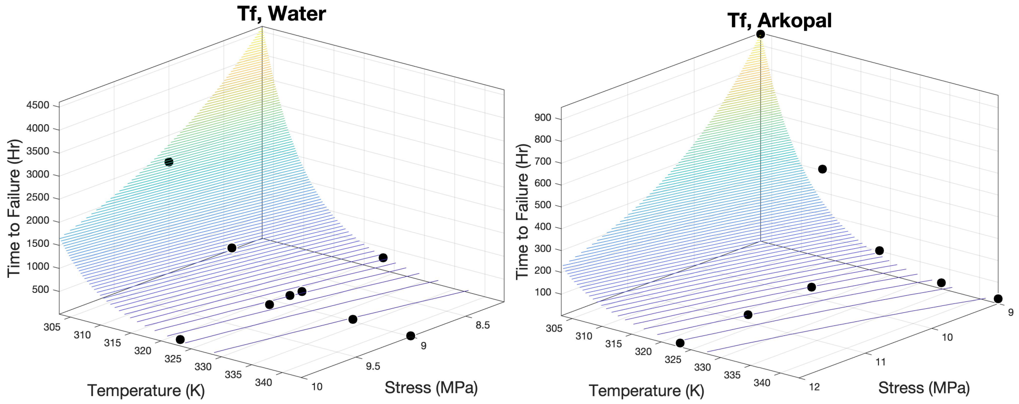

(a) Water (b) Arkopal

Figure 17: 3D contour of time to failure

3.3 Prediction of Brown's SENT experiment using the proposed SCG model: Validation study

The validation of the proposed model was done by using the experimental data of Brown et al. with a single-edge notch test (15). In this case, geometry condition is Y = 2.6, Young's modulus is 1GPa, Poisson's ratio is 0.35, initial COD is $\delta_0 = 15\mu\text{m}$, primordial thickness is $\text{d}_0 = 7.5\mu\text{m}$, and the viscosity is $3 \times 10^{11}\text{Pa} \cdot \text{s}$ (15).

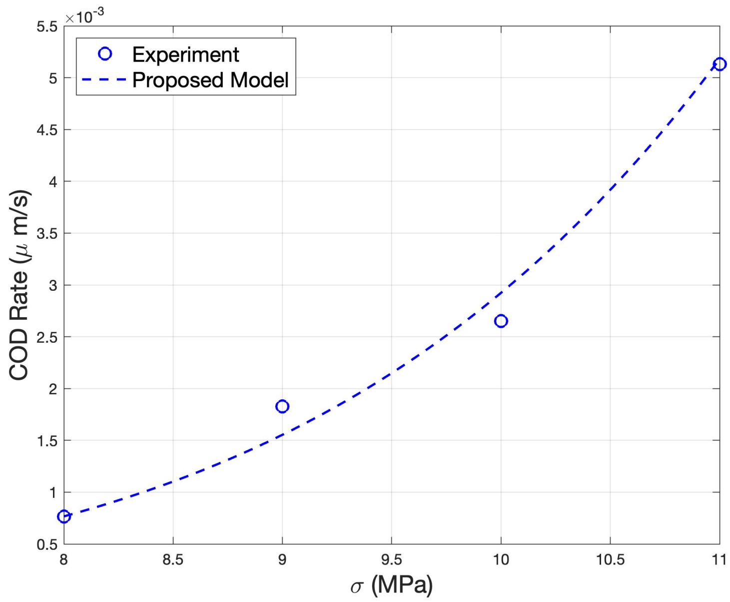

Figure 18: COD rate with SENT specimen (15)

The result from validation also shows a good agreement with experimental data.

4 Conclusion and Future work

The slow crack growth model explaining the thermal and chemical effects was developed. Finite element analysis was conducted to establish the relationship between elongation and crack-tip opening distance so that we can use Schiling's measurement data of total elongation of specimen (9). Our model shows a fair agreement with the experimental data from multiple literature. However, a more physics informed degradation parameters can be used to improve the versatility of current work, that will be valid for any type of chemical degradation when different chemicals are used. Another limitation in the current SCG model is that there is no calibration regarding various initial crack depths even though it plays a significant role in SCG.

In future work, further experimental validation with different specimens with various initial crack depth and chemicals will be helpful to strengthen the proposed SCG model. Also, it will be ideal to develop a theoretical framework for damage based model in semi-crystalline polymer.

[1] A. Lustiger, et al. (1983) Importance of tie molecules in preventing polyethylene fracture under long-term loading conditions, Polymer (Guildf).

[2] N. C. Paxton, et al. (2019) Biomedical applications of polyethylene, European Polymer Journal.

[3] J. J. Han, et al. (2014) Failure assessment diagram analysis of high density polyethylene pipes, Journal of Mechanical Science and Technology.

[4] H. B. H. Hamouda, et al. (2001) Creep damage mechanisms in polyethylene gas pipes, Polymer.

[5] A. Almomani, et al. (2023) Recent advances in slow crack growth modeling of polyethylene materials, Material and Design.

[6] P. Hutar, et al. (2011) A numerical methodology for lifetime estimation of HDPE pressure pipes, Engineering Fracture Mechanics.

[7] M. Schilling (2020) Environmental Stress Cracking (ESC) and Slow Crack Growth (SCG) of PE-HD induced by external fluids, Darmstadt Technical University.

[8] M. Thuy, et al. (2022)Environmental Stress Cracking of High-Density Polyethylene Applying Linear Elastic Fracture Mechanics, Polymers

[9] M. Schilling, et al. (2017) Full notch creep test (FNCT) of PE-HD - Characterization and differentiation of brittle and ductile fracture behavior during environmental stress cracking (ESC), Polymer Testing.

[10] X. Lu, et al. (1988) Slow fracture in a homopolymer and copolymer of polyethylene, Journal of Materials Science.

[11] ASTM D1693-21 (2021) Standard Test Method for Environmental Stress-

Cracking of Ethylene Plastics, American Society for Testing and Materials International.

[12] A. L. Ward, et al. (1990) Accelerated Test for Evaluating Slow Crack Growth of Polyethylene Copolymers in lgepal and Air, Polymer Engineering and Science.

[13] A. Lu (2022) Response and Failure Behavior of HDPE and UHMWPE under Chemical, Biological, and Thermal Environments, Brown University.

[14] N. Brown, et al. (1995) A fundamental theory for slow crack growth in polyethylene, Polymer.

[15] N. Brown, et al. (1991) Slow crack growth in polyethylene - A review, Macromolecular Symposia.

[16] M. Amjadi, et al. (2021) Creep behavior and modeling of high-density polyethylene, Polymer Testing.

[17] H. Riedel. (1977) A Dugdale Model for Crack Opening and Crack Growth under Creep Conditions, Material Science and Engineering.